

Weak ferromagnetism and field-induced spin reorientation in $K_2V_3O_8$

M.D. Lumsden¹, B.C. Sales¹, D. Mandrus^{1,2}, S.E. Nagler¹, and J.R. Thompson^{1,2}

¹ Oak Ridge National Laboratory, P.O. Box 2008, Oak Ridge, TN, 37831 U.S.A.

² Department of Physics, University of Tennessee, Knoxville, TN, 37996-1200 U.S.A.

Magnetization and neutron diffraction measurements indicate long-range antiferromagnetic ordering below $T_N=4$ K in the 2D, $S=1/2$ Heisenberg antiferromagnet $K_2V_3O_8$. The ordered state exhibits “weak ferromagnetism” and novel, field-induced spin reorientations. These experimental observations are well described by a classical, two-spin Heisenberg model incorporating Dzyaloshinskii-Moriya interactions and an additional c-axis anisotropy. This additional anisotropy can be accounted for by inclusion of the symmetric anisotropy term recently described by Kaplan, Shekhtman, Entin-Wohlman, and Aharony. This suggests that $K_2V_3O_8$ may be a very unique system where the *qualitative* behavior relies on the presence of this symmetric anisotropy.

75.25.+z,75.30.-m,75.30.Gw

One of the most exotic and intriguing anisotropies which can occur in magnetic solid state systems is the antisymmetric Dzyaloshinskii-Moriya (DM) interaction. These interactions, originally proposed by Dzyaloshinskii [1] and later derived by Moriya [2] through extension of Anderson’s superexchange model [3], arise from spin-orbit coupling in the presence of sufficiently low local lattice symmetry. The form of this interaction is typically written $\mathbf{D} \cdot (\mathbf{S}_1 \times \mathbf{S}_2)$ where \mathbf{D} is a vector determined by the symmetry of the lattice. Competition between the vector product in the DM interaction and the scalar product in the Heisenberg interaction often leads to novel phenomena such as spin-canting [4] and spiral spin structures [5–8].

Relatively recently, Kaplan [9], and later Shekhtman, Entin-Wohlman, and Aharony (KSEA) [10–12] (motivated by relevance to parent compounds of high- T_c superconductors), re-examined the DM interaction with particular emphasis on an often ignored symmetric component. This symmetric anisotropy always accompanies the typical antisymmetric DM term but is typically ignored as its strength is an order of magnitude weaker. KSEA showed that, in the general case where there is no *frustration*, this symmetric term cannot be ignored as its inclusion restores the original $O(3)$ symmetry of the Heisenberg Hamiltonian. We report in this letter the novel properties of a $S=1/2$, 2d Heisenberg system, $K_2V_3O_8$, and suggest that they can be explained by a model including both symmetric and antisymmetric DM interactions. This implies that $K_2V_3O_8$ is a novel system where the *qualitative* behavior relies heavily on inclusion of the symmetric component of the DM interaction.

$K_2V_3O_8$ crystallizes in a tetragonal unit cell with space group $P4bm$ and lattice constants $a=8.870$ Å and $c=5.215$ Å [13]. The structure is shown in Fig. 1(a) and consists of magnetic V^{4+} - O_5 pyramids and non-magnetic V^{5+} - O_4 tetrahedra with interstitial K^+ ions. Previous magnetic measurements consisted of powder magnetization from 5–300 K [14] which were best described by a 2D Heisenberg model with coupling constant $J=12.6$ K and

a g-value of 1.89. EPR measurements on single crystals suggest very small anisotropy with g-values of $g_c=1.922$ and $g_{ab}=1.972$ [15]. Liu et al. [14] suggested from observation of field-dependent magnetization that $K_2V_3O_8$ may order at lower temperatures.

Single crystal plates of $K_2V_3O_8$ (typical dimensions: $1 \times 1 \times 0.1$ cm³) were grown in a platinum crucible by cooling appropriate amounts of VO_2 in a molten KVO_3 flux. Additional details of the crystal growth will be reported elsewhere. [16] One of these single crystals was mounted in a Quantum Design SQUID magnetometer equipped with a sample rotator and the magnetization is shown in Fig. 2 as a function of both temperature (a) and applied magnetic field (b) for fields applied along both the c-axis and within the tetragonal basal plane. The $M(T)$ data (Fig. 2(a)) were measured by cooling in the presence of an applied magnetic field while the $M(H)$ data (Fig. 2(b)) were taken by cooling to base temperature in zero-field. From Fig. 2(a), the magnetization is seen to be very isotropic for temperatures in excess of about 8 K confirming the Heisenberg nature of the interactions. At high temperatures, we observe a Curie-Weiss susceptibility with an effective moment ($\mu = g\mu_B[S(S+1)]^{1/2}$) of $1.7\mu_B$ per formula unit (FU). This result is consistent with the presence of two non-magnetic V-ions per FU and one magnetic ion with $S=1/2$.

The temperature dependence in the presence of a weak magnetic field shows a clear ordering phase transition below a temperature of about 4 K. The rapid decrease of the magnetization below this temperature with field applied along the c-axis is indicative of antiferromagnetic ordering state with an easy axis along c. However, measurements within the basal plane show a clear ferromagnetic enhancement upon entering the ordered state. The ferromagnetic ordered moment is small ($\sim 10^{-2} \mu_B$) and thus we conclude that the system is antiferromagnetic with spins primarily along the c-axis and a small canted moment in the basal plane. This represents the first observation of an ordering phase transition in this material.

The behavior of the magnetization as a function of

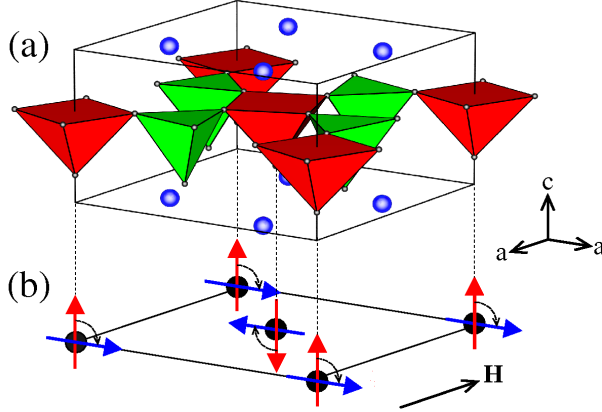


FIG. 1. (a) The crystal structure of $\text{K}_2\text{V}_3\text{O}_8$ composed of magnetic $\text{V}^{4+}\text{-O}_5$ pyramids and non-magnetic $\text{V}^{5+}\text{-O}_4$ tetrahedra. (b) The projection of the V^{4+} positions showing the location of the magnetic moments. The red arrows represent the zero-field spin configuration and the blue arrows denote the behavior of the system in the presence of a basal plane magnetic field (in the direction shown by \mathbf{H}).

field for temperatures well below the Néel temperature is shown in Fig. 2(b). For field applied along c , we observe an abrupt increase in magnetization for fields in excess of about 0.85 T consistent with a discontinuous spin-flop phase transition, further confirming the easy nature of the c -axis. For fields within the basal plane, we observe an intriguing field-induced phase transition which occurs at a magnetic field of $H_{SR}=0.65$ T. There was no evidence of irreversibility in $M(H)$ for either field orientation or in angular rotations of the sample in the presence of an applied field and no evidence of thermal hysteresis was observed.

To investigate the detailed microscopic spin arrangement, neutron diffraction measurements were performed on the HB1A and HB1 triple axis spectrometers at the High Flux Isotope Reactor in Oak Ridge National Laboratory. For the measurements in zero-field, the sample was mounted in the $(h0l)$ scattering plane and comparison of scattering at 1.6 K and 10 K indicated the presence of magnetic Bragg peaks (in the $(h0l)$ plane) described by integer indices with h odd. These peaks suggest a magnetic unit cell in which the corner and face-center moments within the basal plane are aligned antiparallel with parallel alignment along the c -axis. Examination of the integrated intensities of 6 magnetic reflections indicated that the moments lie along the c -axis consistent with conclusions drawn from the magnetization measurements. The value of the ordered moment ($\mu=g\mu_B S$) was found to be $0.72(4) \mu_B$ at $T=1.6$ K, reduced from the expected value of $1 \mu_B$. This can likely be attributed to quantum fluctuations in the low-dimensional $S=1/2$ system. The zero-field magnetic structure is shown schemat-

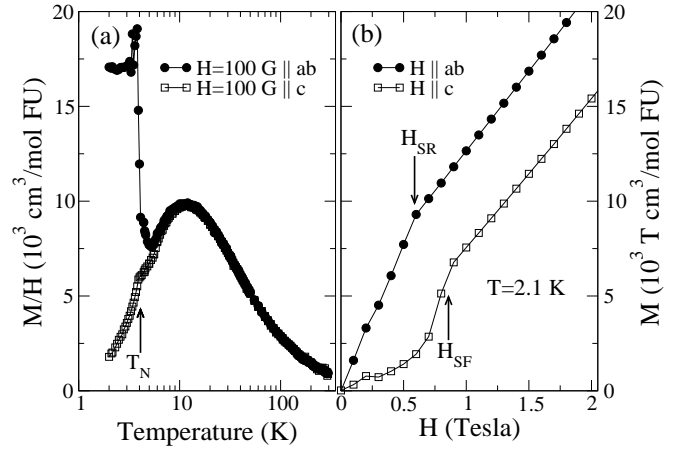


FIG. 2. (a) The temperature dependence of the DC susceptibility in a small applied magnetic field. For temperatures in excess of about 8 K, the system is seen to be very isotropic. Below 4 K, the system undergoes a phase transition to an antiferromagnetic state characterized by an *easy* c -axis and weak ferromagnetic behavior in the basal plane. (b) The magnetization as a function of applied magnetic field for temperatures well below the ordering temperature. Field-induced phase transitions are observed for field applied in the basal plane (H_{SR}) and along the c -axis (H_{SF}).

ically by the red arrows in Fig. 1(b).

To examine the behavior in the presence of a basal plane magnetic field, the crystal was mounted in the $(h0l)$ scattering plane and a vertical field applied along the (010) direction. The field dependence of the (100) and (101) magnetic Bragg peaks are shown in Figs. 3(a) and 3(b). As the intensity of magnetic neutron scattering is proportional to the component of magnetic moment normal to the wavevector transfer, Q , the observed disappearance of the (100) magnetic Bragg peak and the concomitant enhancement of the (101) reflection are consistent with a continuous rotation of the spins from the (001) to the (100) direction with increasing magnetic field strength. The rotation is complete at a field strength of $H_{SR}=0.65$ T in excellent agreement with the anomaly in the magnetization. This is shown schematically by the blue arrows in Fig. 1(b). Thus, we conclude that this transition is a peculiar spin-reorientation phase transition whereby the spins rotate from the c -axis to the basal plane while remaining normal to the applied field direction.

A second crystal was mounted in the $(hk0)$ scattering plane to allow measurements with field applied along the c -axis. The results of these measurements are shown in Fig 3(c) and (d). As a function of applied magnetic field, the (100) Bragg peak intensity drops abruptly upon passing through a field of 0.85 T suggesting a discontinuous reorientation of the spins. The temperature dependence in an applied field of 1 T shows a strikingly different behavior for the (100) and (010) Bragg peaks and

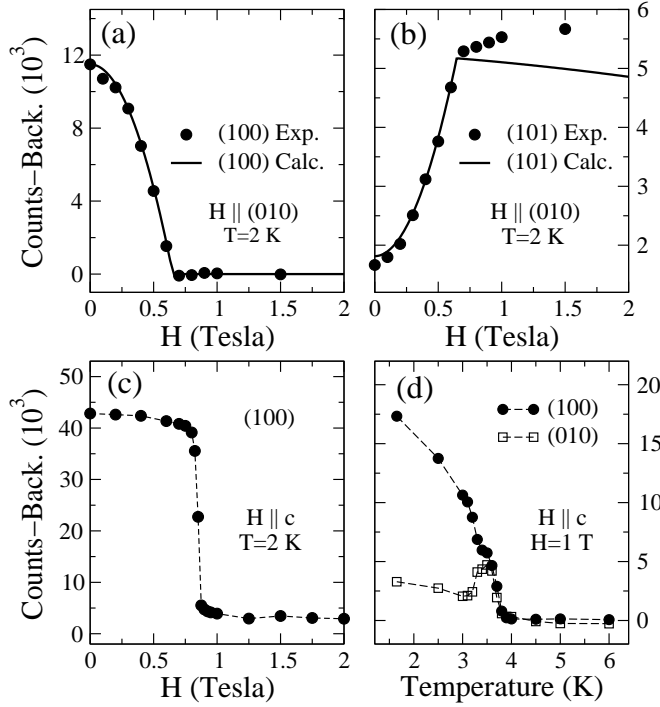


FIG. 3. The background subtracted intensity of diffracted neutrons as a function of applied magnetic field (along the (010) direction), for temperature well below the Néel temperature, is shown for the (100) and (101) magnetic Bragg peaks in panels (a) and (b). The solid lines represent calculations based on the model described in the text. (c) The field dependence of the (100) Bragg reflection with field applied along the c-axis, for temperature well below the ordering temperature, showing a discontinuous spin-flop phase transition. (d) The temperature dependence of (100) and (010) in an applied field of 1 T.

the weaker intensity for (010) suggests that the moments have “flopped” from the c-axis into the basal plane selecting a specific direction within the basal plane in close proximity to the (010) direction. No evidence for a structural distortion has been observed and the selection of a specific direction likely results from a slight misalignment of the magnetic field with the c-axis. This misalignment was less than 1° for the measurements performed but even this level may induce a net field in the basal plane of sufficient strength to overcome domain energies thus selecting a specific magnetic domain. Such a domain selection has been observed in the tetragonal antiferromagnet MnF_2 [17].

As mentioned in the introduction, weak ferromagnets often have at their origin the competition between the antisymmetric DM interaction and the symmetric Heisenberg interaction. To consider the DM interactions in $\text{K}_2\text{V}_3\text{O}_8$, we will consider the projection of the crystal structure onto the tetragonal basal plane as shown in Fig. 4(a). The plane of inversion symmetry between near-neighbor V^{4+} spins results in DM vectors located in that

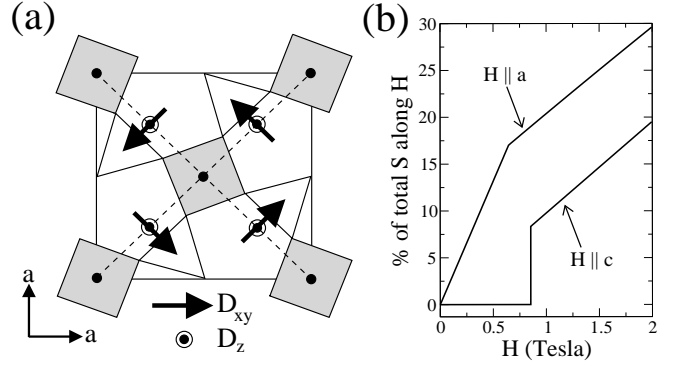


FIG. 4. (a) The projection of the crystal structure onto the tetragonal basal plane. The magnetic moments are located at the center of the shaded squares and the triangles represent the $\text{V}^{5+}\text{-O}_5$ tetrahedra. The components of the Dzyaloshinskii-Moriya vectors (\mathbf{D}_{xy} and \mathbf{D}_z) are shown in the figure relative to the central spin. (b) The calculated component of magnetic moment along the field direction as a function of applied field for field applied along both a and c. This result compares very well to the $M(H)$ data plotted in Fig. 2(b).

inversion plane [4] giving components along (110) and (001) directions, denoted by \mathbf{D}_{xy} and \mathbf{D}_z respectively (these directional vectors are indicated in the figure relative to the central site). The four-fold rotation symmetry through the central site gives rise to the configuration of \mathbf{D} vectors shown in the figure. From the neutron diffraction measurements, we know that the magnetic unit cell contains two spins in both zero and non-zero fields and, hence, we will consider a two-spin, classical Hamiltonian. Noting that in averaging over the near-neighbor spins within a unit cell, the components of the DM vectors in the basal plane (i.e. the \mathbf{D}_{xy} terms) cancel, we write the ground state energy as

$$F = J\mathbf{M}_1 \cdot \mathbf{M}_2 + D_z[\mathbf{M}_1 \times \mathbf{M}_2]_z \quad (1)$$

where \mathbf{M}_1 and \mathbf{M}_2 are the sublattice magnetizations and $[\mathbf{M}_1 \times \mathbf{M}_2]_z$ is the z-component of the vector cross-product.

This ground state energy will be minimized when the spins are in the basal plane and, consequently, an additional c-axis anisotropy is required to account for the easy c-axis observed experimentally. Thus, we add a c-axis anisotropy of the form $E_z M_{1z} M_{2z}$ and, with addition of the Zeeman energy for nonzero field, we arrive at the ground state energy,

$$F = J\mathbf{M}_1 \cdot \mathbf{M}_2 + D_z[\mathbf{M}_1 \times \mathbf{M}_2]_z + E_z M_{1z} M_{2z} + g\mu_B \mathbf{H} \cdot [\mathbf{M}_1 + \mathbf{M}_2]. \quad (2)$$

This rather simple, classical ground state energy describes all the low temperature properties of the system. For appropriate values of D_z and E_z , the spins will point along the c-axis with canting observed in small fields due

to the normal competition between DM and Heisenberg interactions. For fields applied in the basal plane, the Zeeman energy and the DM interaction favor arrangement of the spins in the basal plane. This competes with the c-axis anisotropy causing a continuous rotation of the spins to the basal plane with increasing field strength. The spins remain primarily normal to the applied field direction to minimize the Zeeman energy. Finally, with field applied along the c-axis, a spin-flop transition occurs due to competition between Zeeman energy and the anisotropies in the system causing an abrupt rotation of the spins into the basal plane.

As we have two field-induced phase transitions, we can estimate the values for D_z/J and E_z/J required to produce phase transitions at the measured field values (using $J=12.6\text{K}$ and $g=1.89$ as determined from Liu et al. [14]). This results in a value of $D_z/J=0.22$ and $E_z/J=3.8\times 10^{-2}$ (this value of D/J seems large considering the measured g -values [14,15] but compares favorably to the DM spiral system $\text{BaCuGe}_2\text{O}_7$ which has a similar basal plane structure and for which D/J was found to be ~ 0.18 [8]). Using these values, we can calculate the induced magnetic moment along the field direction for field applied along both the a - and c -axes and the results are plotted in Fig. 4(d) as a function of applied magnetic field in Tesla. These results can be directly compared to the $M(H)$ data plotted in Fig. 2(b) and the qualitative agreement is remarkable suggesting that this relatively simple model adequately describes the low temperature properties of the system. To further emphasize this, we have superimposed on Fig. 3(a) and 3(b) the calculated magnetic Bragg peak intensity for the (100) and (101) reflections in the presence of an applied magnetic field along the (010) direction. These results are represented by the solid lines in Figs. 3(a) and 3(b) and the agreement between the calculations and the data is excellent, particularly for the (100) reflection. The agreement for the (101) reflection is very good for field strengths up to H_{SR} but seems to deviate for higher fields. The reason for this disagreement is unclear but could result from a field-dependent $\langle S \rangle$. Such a scenario can occur via field-dependent suppression of quantum fluctuations, as has been observed in some ABX_3 antiferromagnets [18].

To shed some light on the nature of the c -axis anisotropy, we calculate the symmetric anisotropy term of KSEA. The addition of this term causes a rescaling of J to $(J-D^2/4J)$ and the inclusion of a symmetric anisotropy term $(1/2J)\mathbf{M}_1\cdot\mathbf{A}\cdot\mathbf{M}_2$ where \mathbf{A} is a 3×3 matrix with elements $A_{uv}=D_uD_v$ [11,19]. Making these changes to the Hamiltonian and averaging over near-neighbor spins produces the ground state energy,

$$F = (J - \frac{D_z^2}{4J})\mathbf{M}_1 \cdot \mathbf{M}_2 + D_z[\mathbf{M}_1 \times \mathbf{M}_2]_z + (\frac{D_z^2}{2J} - \frac{D_{xy}^2}{4J})M_{1z}M_{2z} + g\mu_B\mathbf{H} \cdot [\mathbf{M}_1 + \mathbf{M}_2]. \quad (3)$$

This energy has precisely the same form as Eq. 2 and, consequently, the c -axis anisotropy falls out naturally upon inclusion of both the symmetric and antisymmetric anisotropies. The maximum value for the c -axis anisotropy in Eq. 3 is $D_z^2/2J$ which, for D_z/J of 0.22, gives a maximum anisotropy (E_z/J) of 2.4×10^{-2} . Within the level of approximation involved in this model, this is in reasonably good agreement with the above value of 3.8×10^{-2} . Consequently, we conclude that $\text{K}_2\text{V}_3\text{O}_8$ represents a unique system where the *qualitative* features rely heavily on the inclusion of the KSEA symmetric anisotropy term. The only known, clear evidence of this symmetric anisotropy occurs in the DM spiral system $\text{Ba}_2\text{CuGe}_2\text{O}_7$ where the addition of this term is necessary to produce *quantitative* agreement between experiment and theory [20]. As a caveat, it is important to note that we cannot rule out other possible mechanisms for this additional anisotropy. Rather, we simply note that inclusion of this symmetric anisotropy alone, which is necessary to properly consider DM interactions, seems to adequately describe the properties of the system.

In summary, we have observed an ordering phase transition in $\text{K}_2\text{V}_3\text{O}_8$ with a primarily antiferromagnetic ordered state accompanied by weak ferromagnetism. Field-induced spin reorientation phase transitions have been observed with field applied along both the c -axis and in the tetragonal basal plane. The spin arrangement has been determined by single-crystal neutron diffraction measurements. Remarkably, this rich magnetic behavior can be well described by a simple, classical, two-spin Heisenberg model with inclusion of DM interactions and an additional c -axis anisotropy. This additional anisotropy can, at least partially, be accounted for by inclusion of the KSEA symmetric anisotropy term making $\text{K}_2\text{V}_3\text{O}_8$ a unique system where introduction of this interaction is necessary to describe the *qualitative* behavior of the system.

We would like to acknowledge stimulating discussions with G. Murthy, M.W. Meisel, R. Coldea, and D.A. Tennant. Oak Ridge National Laboratory is managed by UT-Battelle, LLC, for the U.S. Dept. of Energy under contract DE-AC05-00OR22725.

-
- [1] I. Dzyaloshinskii, Sov. Phys. JETP **5**, 1259 (1957).
 - [2] T. Moriya, Phys. Rev. **120**, 91 (1960).
 - [3] P.W. Anderson, Phys. Rev. **115**, 2 (1959).
 - [4] See for example, T. Moriya, in *Magnetism I*, Edited by George T. Rado and Harry Suhl (Academic Press, New York, 1963) and references therein.
 - [5] Y. Ishikawa *et al.*, Phys. Rev. B **16**, 4956 (1977).
 - [6] Y. Ishikawa and M. Arai, J. Phys. Soc. Jpn. **53**, 2726 (1984).

- [7] B. Lebech *et al.*, J. Phys. Condens. Matter **1**, 6105 (1989).
- [8] A. Zheludev *et al.*, Phys. Rev. B **56**, 14006 (1997).
- [9] T.A. Kaplan, Z. Phys. B **49**, 313 (1983).
- [10] L. Shekhtman, O. Entin-Wohlman, and A. Aharony, Phys. Rev. Lett. **69**, 836 (1992).
- [11] L. Shekhtman, A. Aharony, and O. Entin-Wohlman, Phys. Rev. B **47**, 174 (1993).
- [12] O. Entin-Wohlman, A. Aharony, and L. Shekhtman, Phys. Rev. B **50**, 3068 (1994).
- [13] J. Galy and A. Carpy, Acta. Cryst. **B31**, 1794 (1975).
- [14] Guo Liu and J.E. Greedan, J. Solid State Chem., **114**, 499 (1995).
- [15] M. Pouchard *et al.*, Bull. Soc. Chim. Belg. **97**, 241 (1988).
- [16] B.C. Sales, unpublished.
- [17] G.P. Felcher and R. Kleb, Europhys. Lett. **36**, 455 (1996).
- [18] A.S. Borovik-Romanov *et al.*, JETP Lett. **66** 759 (1997).
- [19] T. Yildirim *et al.*, Phys. Rev. B **52** 10239 (1995).
- [20] A. Zheludev *et al.* Phys. Rev. Lett. **81**, 5410 (1998).